
Impact of Cast Iron Degradation and Cathode Block Erosion on the Current Path in the Cathodic Assembly of Aluminum Production Cells

Martin Brassard, Marc LeBreux, Martin Désilets, Gervais Soucy, Martin Forté, and Jean-François Bilodeau

Abstract

Carbon-cast iron electrical contact degradation is still considered as one of the main cause for the CVD increase over the lifetime of the electrolysis cell. A thermoelectric finite element model was developed to evaluate the effect of the carbon-cast iron electrical contact degradation and the cathode erosion on the CVD and the current distribution inside the cathodic assembly. Chemical degradation data from laboratory and industrial samples were used to calibrate the cast iron and the contact resistivities. Results demonstrate that the carbon block erosion and the contact degradation at the cast iron interface have a direct impact on the current distribution at the carbon block surface. Both factors increase the CVD when taken separately but the contact degradation outperforms the carbon block wear when taken together.

Keywords

Aluminum • Cathode • Carbon • Cast iron • Degradation • Erosion • CVD

Introduction

The cathode voltage drop (CVD) accounts for about 8% of the total voltage of the aluminum production cell [1]. This energy loss needs to be kept as low as possible to optimize the production cost. The CVD is known to increase over the cell's life [2, 3]. One of the identified cause is the degradation of the cast iron surface used to make the connection between carbon block and the steel collector bars. That being said, other phenomena at the carbon block surface like erosion may also have an effect [4].

This study is an extension of the studies on cast iron degradation mechanisms that have been already conducted and published [5]. Further investigations about the

relationship between the cast iron electrical contact degradation and the carbon block wear are carried out using a finite element thermoelectric model built within ANSYS software.

Methodology

Collector Bar Autopsy

One complete collector bar was extracted from a 2500 days old aluminum production cell. The cast iron cylinders were recovered using a two-steps operation: surface was drilled using a diamond grit hole saw to cross the surface deposit and the remaining cast iron was cut using a carbide grit hole saw. After resin mounting, the extracted cylinders were cut in half and polished to conduct metallography analysis.

The optical microscope images of the surface deposit were transformed into binary images. The white areas were considered as metallic phases while the black areas were

M. Brassard · M. LeBreux · M. Désilets · G. Soucy (✉)
Université de Sherbrooke, 2500, Boulevard de L'Université,
Sherbrooke, Québec, J1K 2R1, Canada
e-mail: gervais.soucy@usherbrooke.ca

M. Forté · J.-F. Bilodeau
Rio Tinto (Centre de Recherche et Développement D'Arvida),
P.O. Box 1250, Saguenay, Québec, G7S 4K8, Canada

Table 1 Metallic fraction and thickness of the cast iron surface deposit

	Metallic fraction	Deposit thickness (mm)
Top of the collector bar	0.6	2.1
Side of the collector bar	0.5–0.75	1.1
Outer end section	0.05	2–7.5

interpreted as a mixture of electrolytic bath. Table 1 gives the consolidated data of the surface of the collector bar.

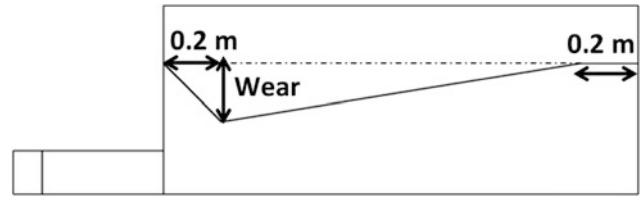
The deposit was considered as a metal foam in order to estimate resistivity increase due to the surface deposit as compared to the cast iron. The calculations were done using the Eq. 1, x_m being the metallic fraction, ρ_{mix} being the deposit resistivity and ρ_{CI} being the cast iron resistivity.

$$\frac{\rho_{mix}}{\rho_{CI}} = \frac{1}{(x_m)^{3/2}} \quad (1)$$

Thermoelectric Finite Element Model

In order to predict the effect of the cathode wear on the CVD and the distribution of current density on the cathode block, a three dimensional coupled thermoelectric finite element model of the cathode block assembly is built with ANSYS. In the proposed work the finite element model is solved for steady-state regime only. Moreover, due to the symmetry conditions, only a quarter of the geometry is studied. A schematic of the proposed model is shown in Fig. 1.

The collector bar is made out of carbon steel rod in cast iron. An additional layer of cast iron is added to the model to represent the addition of a reactive layer that forms due to chemical degradation of the contact area. The shape of the groove in the carbon block is rectangular and the contact is considered to be perfect between the carbon and the cast iron [6]. The cathode block is assumed to be made of graphitized carbon. The erosion of the carbon block is also

**Fig. 2** Schematic of the cathode wear profile

taken into account by modifying the cathode geometry, following the schematic of Fig. 2. The wear pattern is based on previous published results on a related technology [7]. In this work, only the wear depth is modified, it varies from 0 to 0.25 m. On the top of the carbon block, a “pseudomaterial” is used to mimic the behavior of molten aluminum metal in the center of the cell and that of the solid ledge on the side.

The governing equations for the electrical potential distribution and energy conservation may then be stated as [8]:

$$\nabla[\sigma(T)\nabla V] = 0 \quad (2)$$

$$\nabla[k(T)\nabla T] + \ddot{q} = 0 \quad (3)$$

where σ is the electrical conductivity, V is the electrical potential, k is the thermal conductivity and T the temperature. As can be seen in Eqs. 2–3, the electric and thermal conductivities are function of the temperature. Moreover, the volumetric heat source term \ddot{q} represents the Joule effect caused by the electric current flowing into the cathode block assembly:

$$\ddot{q} = \sigma E^2 \quad (4)$$

where the electrical field is obtained from the solution of Eq. 2 for the electric potential V . The corresponding boundary conditions are summarized in Table 2.

For a chosen cathode wear profile (Fig. 2), the set of boundary conditions (Table 2), and the thermoelectric properties of each material (k , σ), the system of Eqs. 2–4 is

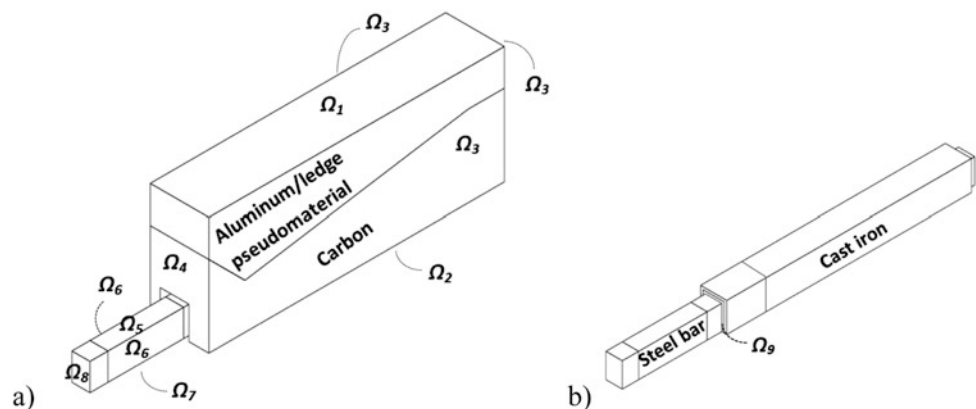
Fig. 1 Schematic of the **a** cathode block assembly and **b** the cast iron layers wrapping the steel collector bar

Table 2 Boundary conditions of the finite element model

Boundary	Boundary conditions
Ω_1	Fixed voltage, fixed temperature
$\Omega_2, \Omega_4, \Omega_5, \Omega_6, \Omega_7$	Convection heat transfer
Ω_3	Symmetry for heat transfer and electric current
Ω_8	Fixed current
Ω_9	Fixed electric contact resistance at steel/cast iron interface

solved using ANSYS Mechanical software (release 16.0). In this case, calculations are performed within the cathode block assembly using a grid size of 375 000 nodes. Convergence is declared when the sum of residuals for the distribution of the electrical potential as well the temperature is inferior to 0.1%.

Results and Discussion

Estimation of the Surface Deposit Electrical Resistivity

The surface deposit resistivity increase is estimated according to the data that are displayed in the Table 1 and in Eq. 1. The results displayed in Table 3 shows that the resistivity increases from 1.5 to 2.8 for most of the cast iron surface except for the outer end section, which presents a much higher increase with a value of 89. Those results have been used to calibrate the model.

Effect of the Wear Profile on the Current Density Distribution

Figure 3 displays the 3D distribution of the current density at the surface of the cathode block, for each wear profile. It shows also the current density distribution at the cast iron upper surface. On top of the cathode, the current density concentrates at the ledge toe. Temperature results of the

Table 3 Increase of resistivity of the cast iron surface relative to the virgin cast iron

	Resistivity increase estimation
Top of the bar	2.15
Side of the bar	1.5–2.8
Outer end section	89

finite element model have shown that as the erosion goes deeper in the carbon block, the ledge toe becomes thicker. By being an electric insulator, it pushes the current density toward the center of the block where the surface is free of deposit.

Effect of the Cast Iron Electrical Contact Degradation Combined with the Wear Profile on the Current Density Distribution

The cast iron resistivity was updated in the model according to the data presented in Table 3. The modified model parameters are displayed in Table 4. The cast iron layer thickness in the model is 15 mm, which is by far thicker than the surface deposit observed in the collector bar autopsy (1–2 mm). Previously reported results have shown that the cast iron resistivity increases by two folds causes an increase of 1% on the CVD [5]. However, in the same study, calculations have shown that the contact resistivity increase has a much greater effect on the CVD. The contact resistivity was increased by 100 folds instead of the cast iron resistivity to maximize the effect of degradation in the model.

Figure 4 displays the 3D distribution of the current density for each wear profile combined with the electrical contact degradation of the cast iron. This figure also presents the current density distribution at the cast iron upper surface. As shown in the previous section, the current density distribution is affected by the wear level of the carbon block. However, one can see that the current density distribution on the carbon block is clearly affected by the cast iron degradation. The effect is the most evident for the carbon block without erosion. In that case, the current density stays below 20,000 A/m² and there is limited current concentration where the ledge toe is located.

Figure 5 presents the maximum current density value and its position along the length of the cathode block for both scenarios of collector bar degradation. Results show that for each wear profile, the current density is higher when the cast iron contact is degraded. In that case, the maximum current density is located at the cast iron surface, but for a wear depth greater or equal than 0.2 m, the maximum current density is now located at the top surface of the cathode. However, when the cast iron contact is not degraded, the maximum current density value is located at the top surface of the cathode for a wear depth greater or equal than 0.05 m. For a cathode which is not eroded (wear = 0 m), the location of the maximum current density is moved to the cast iron surface.

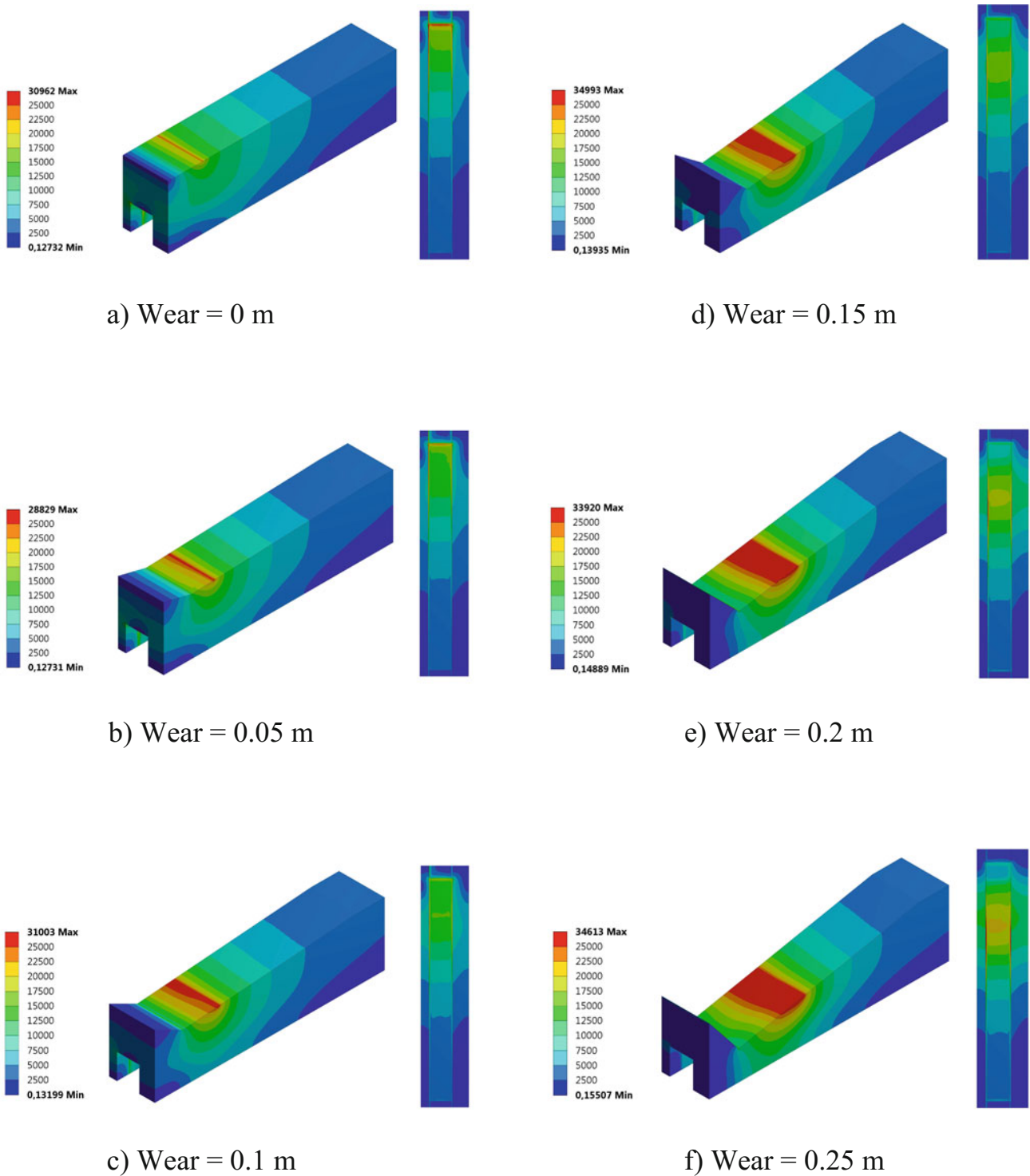


Fig. 3 Effect of the wear profile on the current density distribution—No cast iron degradation

Effect of the Wear Profile on the CVD

Figure 6 shows the CVD variation in relation with the wear level and the degradation of the cast iron. Figure 4 revealed previously that the current density is pushed toward the

center of the block as the wear goes deeper. This causes the current path to be longer and to increase the equivalent resistance according to Ohm’s law.

The CVD behavior is different when the cast iron electrical contact is degraded. In such a case, the CVD does not

Table 4 Cast iron and contact resistivity modification

	Cast iron outer layer resistivity increase ^a	Cast iron to carbon contact resistivity increase
Top of the bar	2	2
Side of the bar	2	2
Outer end	2	100

^aThe outer layer refer to the cast iron layer in contact with the carbon block. See the model geometry for more details

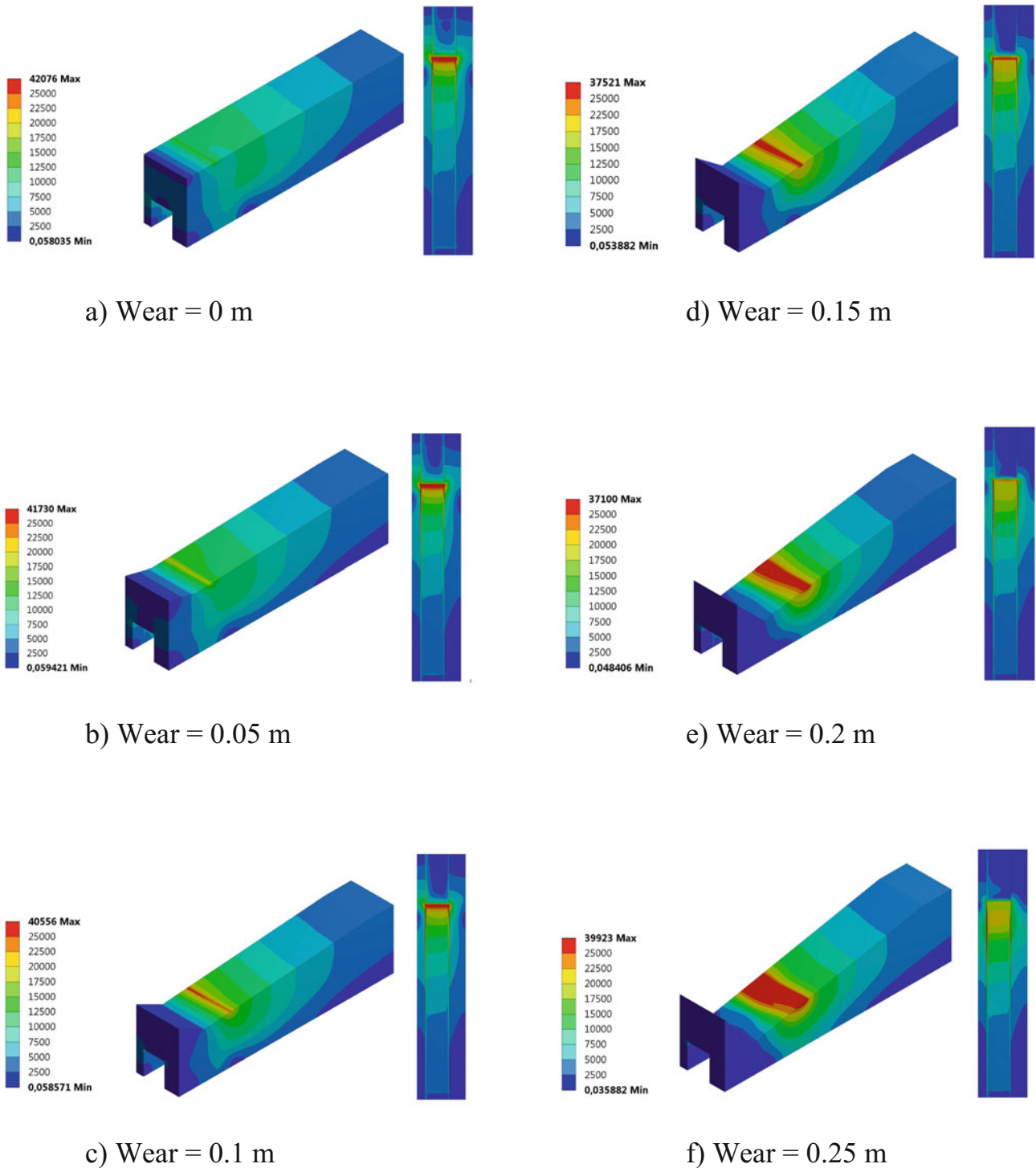


Fig. 4 Effect of the wear profile on the current density distribution—with degradation

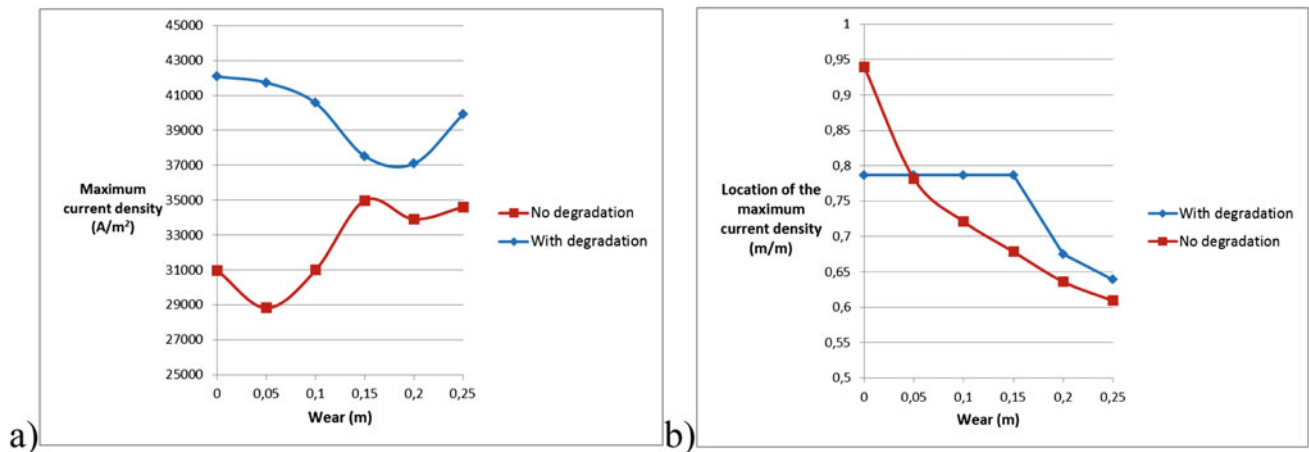


Fig. 5 a Maximum current density value and b its position on the block surface from the inner end of the carbon block

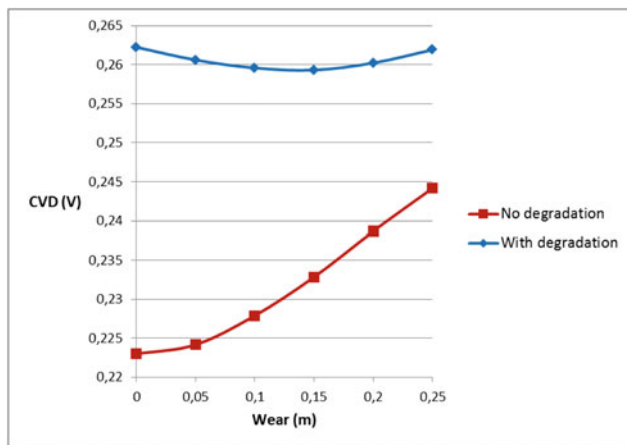


Fig. 6 Effect of the wear profile and cast iron degradation on the CVD

change much in relation with the wear level. The current path is preferentially influenced by the cast iron degradation and the wear has little effect on the final CVD result.

Conclusion

The thermoelectric finite element model developed for this analysis has demonstrated that the current density distribution at the surface of the cathode block is related to the depth of the wear. As the erosion progresses, the current density is moved toward the center of the carbon block. This phenomenon is observed no matter what is the cast iron degradation evolution. However, the maximum current density is moved from the carbon block surface to the cast iron when its degradation is taken into account.

Moreover, the thermoelectric model has shown that the wear by itself can cause an increase on the CVD. Results

have shown that the CVD increased by about 10% for the 0.25 m deep eroded block compared to the new block. When the cast iron degradation data were implemented, the CVD increased by 17%. In that case, the wear profile had no apparent effect on the CVD result.

Acknowledgements Authors want to thank Dr. Alireza Hekmat's for his input on the metallography analysis. They also wish to acknowledge Rio Tinto, the Natural Sciences and Engineering Council of Canada and the "Fonds de Recherche du Québec, Nature et Technologies" for their financial support.

References

1. H. Kvande, W. Haupin, Cell voltage in aluminum electrolysis: a practical approach. *JOM* **52**(2), 31–37 (2000)
2. W. Haupin, Cathode voltage loss in aluminium smelting cells. *Light Met.* 339–349 (1975) (The Metallurgical Society of AIME)
3. C.J. Michel, Evolution of the cathodic ohmic drop during the electrolysis in the aluminium cell. *Light Met.* 989–1003 (1985) (ed. H.O. Bohner, The Minerals, Metals and Materials Society, New York, NY)
4. D. Lombard et al., Aluminium Pechyney experience with graphitized cathode blocks. *Light Met.* 653–658 (1998) (ed. by B. Welch, The Minerals, Metals and Materials Society, San Antonio, TX)
5. M. Brassard, Dégradation chimique de l'interface cathodique carbone-fonte de cellules de production d'aluminium, Ph.D. Thesis, Université de Sherbrooke, 2016, pp. 61–92
6. M. Gagnon et al., Optimization of the cathode collector bar with a copper insert using finite element method. *Light Met.* 621–626 (2013) (ed. B. Sadler, The Minerals, Metals and Materials Society, San Antonio, TX)
7. P. Reny, S. Wilkening, Graphite cathode wear study at Alouette. *Light Met.* 399–404 (2000) (ed. R.D. Peterson, The Minerals, Metals and Materials Society, Nashville, TN)
8. ANSYS Inc., *ANSYS Mechanical APDL Theory Reference* (Canonburg, PA, 2013)